ORIGINAL RESEARCH

Identification of a Gene Expression Signature to Predict the Risk of Abdominal Aortic Aneurysm in Psoriasis Patients

Xintong Lyu, Qingti Tang, Yu Zou, Xiaorong Liu

Department of Dermatology, Affiliated Hospital of Chengdu University, Chengdu, Sichuan, People's Republic of China

Correspondence: Xintong Lyu, Department of Dermatology, Affiliated Hospital of Chengdu University, 82 North Second Ring Road, Chengdu, 610081, Sichuan, People's Republic of China, Email Xintong_lyu@163.com

Background: : Psoriasis is an immune-mediated, hereditary condition that presents itself in the skin or joints, or even both. Increasing evidence indicates that psoriasis is connected to an elevated risk of abdominal aortic aneurysm (AAA), owing to their shared inflammatory pathogenesis. Nevertheless, the interplay between psoriasis and AAA lacks sufficient documentation.

Methods: Through WGCNA and DEGs, psoriasis and AAA phenotype-related genes were identified. Identifying risk genes involved in both psoriasis and AAA involved generating candidate genes by finding the common intersection of hub genes, followed by using LASSO regression. Following this, a nomogram was created to forecast the development of psoriasis alongside AAA, and was then assessed through a ROC curve, DCA, calibration curve, and PR curve. Five algorithms, namely CIBERSORT, ssGSEA, ESTIMATE, MCPcounter, and QuanTIseq, were utilized to assess immune infiltration differences between high and low-risk groups. Simultaneously, we verified the differential gene expression in different tissues.

Results: A total of 1073 psoriasis hub genes and 128 AAA hub genes were generated. A Venn diagram revealed 20 candidate genes that were common to both hub genes of psoriasis and AAA. Of these, six genes (*CCR7, CD3D, GBP5, HCLS1, IL7R*, and *ITGAL*) were identified as risk genes. The gene signature generated by these genes demonstrated high accuracy in predicting psoriasis and AAA. Using five algorithms for immune infiltration analysis, an abundance of inflammatory cells was observed in high-risk subgroups. The above six genes were found to be highly expressed in both psoriasis tissue and abdominal aortic aneurysm tissue.

Conclusions: : The study resulted in the identification of a novel gene signature, including six high-risk genes, that has enhanced our knowledge of the common causes and control mechanisms of psoriasis and AAA. These findings are anticipated to pave the way for promising therapeutic targets in mitigating the comorbidities of cardiovascular disease.

Keywords: psoriasis, abdominal aortic aneurysm, signature, nomogram

Introduction

Psoriasis, recognized as a systemic inflammatory condition, is linked to cardiometabolic comorbidities.[1] Individuals with psoriasis exhibit a heightened prevalence of cardiovascular ailments, encompassing ischemic heart disease, heart failure, peripheral vascular disease, and stroke.[2–4] The elevated susceptibility to cardiovascular events is thought to be connected to the systemic inflammatory pathophysiological mechanism of psoriasis.

Aortic vascular inflammation is crucial in the advancement and growth of aortic aneurysm (AA). Chronic inflammation in the aorta is believed to harm the aortic wall and disrupt the function of vascular smooth muscle cells in blood vessels, caused by the secretion of different enzymes like matrix metalloproteinases and cysteine proteases, along with free radicals from oxidation, cytokines, and other related substances.[5] The aberrant inflammation observed in psoriasis could contribute to aortic injury, thereby predisposing individuals to developing an aortic aneurysm.[6] An increase in aortic inflammation has been observed in patients with psoriasis when analyzed through 18FDG-PET/CT.[7] Currently, only three nationwide cohort studies have revealed the impact of psoriasis on the incidence of AAA. Both Chiu et al and Khalid et al. Indicate that individuals with psoriasis have a higher likelihood of AAA compared to those without the

condition, especially in cases of severe psoriasis, resulting in increased morbidity rates.[8,9] Conversely, DJ et al suggest that psoriasis may not be a standalone risk factor for AAA thorough meta-analysis found that individuals with psoriasis have a higher susceptibility to AAA compared to the general population, and this risk does not escalate with the seriousness of psoriasis.[10] A comprehensive meta-analysis has revealed that patients with psoriasis are more vulnerable to AAAs in comparison to the general population, and the risk does not increase with the severity of psoriasis.[11] Nevertheless, the conclusions of these studies are inconsistent, and whether psoriasis contributes to an increased risk of AAA remains unclear.

The overactivation of the adaptive immune system is central to the pathogenesis of psoriasis.[12] During the initial phases, a variety of cells that cause inflammation, such as plasmacytoid dendritic cells, natural killer T cells, and macrophages, secrete cytokines that stimulate the growth of keratinocytes, boost the production of substances that promote blood vessel formation, and lead to the infiltration of immune cells into the skin that is affected. Similarly, chronic inflammation induced by the infiltration and activation of various immune cells is a critical driver in the development of AAA.[13,14] It is evident that psoriasis and AAA share overlapping pathogenic pathways.[15] Nevertheless, the precise mechanisms explaining the coexistence of these two conditions remain elusive.

In this present investigation, we have developed a gene signature that demonstrates remarkable accuracy in predicting the occurrence of psoriasis with AAA. Additionally, the expression level of this gene signature corresponds to the presence of inflammatory cells within the immune microenvironment of psoriasis. This suggests that the candidate genes could be involved in the extended inflammatory processes linked to both psoriasis and AAA. Simultaneously, we confirmed through basic experiments that the candidate genes are highly expressed in both psoriasis and abdominal aortic aneurysm. Consequently, these findings provide compelling evidence for the exploration of potential therapeutic targets in the treatment of psoriasis and AAA.

Materials and Methods
Data Downloaded and Processing
Obtained gene expression profiles from the Gene Expression Omnibus. A total of ten datasets were included in the analysis: GSE226244, GSE182640, GSE181318, GSE166388, GSE153007, GSE68923 (which also includes GSE68937), GSE78097, GSE79704, GSE63741, and GSE13355, which contained samples from patients with psoriasis. For training purposes, we employed the GSE226244 dataset, while the remaining nine datasets were used for testing. Furthermore, we acquired the GSE57691 dataset, containing 10 normal control samples and 49 AAA samples, for analysis of the training set. Dataset GSE47472, which consists of 8 normal control samples and 14 AAA samples, was ultimately added for analysis of the testing set. Principal component analysis (PCA) was used to assess the distinction between each sample.

Detection of Genes With Altered Expression Levels
RNA probes were re-annotated using the R package 'AnnoProbe'. A comparison of gene expression matrices from psoriasis and AAA samples was conducted using the 'limma' R package. Differential expression analysis was conducted based on the criteria of $|\log2FC| \geq 1$ and adjusted P-value < 0.05. A volcano plot and Venn diagram were created in OmicStudio (https://www.omicstudio.cn/tool) to display the overlapping DEGs in these datasets.

Weighted Gene Co-Expression Network Analysis for Psoriasis and Abdominal Aortic Aneurysm
The system biology approach known as WGCNA was devised to uncover overarching patterns in gene expression and explore the relationships between genes.[16] The Pearson algorithm was used to analyze all gene pairs in order to create a weighted adjacency matrix. Afterward, an appropriate soft-thresholding exponent was chosen by considering the distribution of the scale-free criteria, leading to improved co-expression similarity and aiding in the construction of a scale-free network approximation. The identification of similar modules involved the use of the topological overlap measurement, and the dynamic tree-cutting method was employed to reveal overlapping modules. Finally, the association

between modules and traits was investigated using Pearson correlation analysis. Modules with P values below 0.05 and a correlation exceeding 0.5 were considered noteworthy and utilized for further analysis.

Functional Enrichment Analysis

The Gene Ontology (GO) framework provides a structured format of machine-readable information that details the functions undertaken by genes and their products.[17] Within the GO enrichment analysis, the DEGs acquired from the GSE226244 dataset were selected and processed using the 'clusterProfiler' R package.[18] Scatter plots were used to display the top 30 enhanced results for biological processes, molecular functions, and cellular components, all with a q value less than 0.05, individually.

Gene Set Enrichment Analysis

GSEA is a popular computational tool that evaluates biological processes and pathways by analyzing whether a known set of genes shows significant differences between two different biological conditions.[19] To differentiate the KEGG pathway patterns between the normal and psoriasis skin samples, an enrichment analysis was performed on the GSE226244 dataset using the R package 'clusterProfiler'. In this analysis, a corrected P value with a threshold of < 0.05 was considered indicative of significant statistical differences.Identification of Risk Genes of Abdominal Aortic Aneurysm in Psoriasis.

A Venn diagram was employed to identify shared genes between the DEGs and hub module genes associated with psoriasis and AAA. The overlapping genes were then visualized using a Venn diagram. Afterwards, the online database STRING was used to create the Protein-Protein Interaction (PPI) network for these common genes. In constructing this gene interaction network, each gene was evaluated using network topology parameters. From a pool of intersecting genes, core genes were consequently selected and highlighted using the Xiantao website (https://www.xiantaozi.com/). LASSO regression was additionally utilized to improve the predictive efficiency and comprehensibility of the statistical model through variable selection and regularization methods.[20] Genes linked to risk were identified using LASSO regression.

Evaluation of the Risk Gene Signature in Psoriasis and Abdominal Aortic Aneurysm

To further evaluate the predictive value of these six genes in diagnosing psoriasis and AAA, a gene signature was constructed. The performance of the gene signature in diagnosis was assessed by plotting a receiver operating characteristic (ROC) curve using the 'pROC' R package. The area under the curve (AUC) and its corresponding 95% confidence interval (CI) were calculated, with an AUC greater than 0.7 considered as the threshold for an ideal diagnostic value. A nomogram was created using the 'rms' R package, which incorporated the risk genes.[21] Candidate genes were scored as 'Points', with the sum of these scores referred to as 'Total Points'. Furthermore, a nomoscore was calculated by combining coefficients from logistic regression with the expression levels of hub genes. To comprehensively evaluate the prediction accuracy of the gene signature for AAA diagnosis, various analyses such as precision-recall curve, calibration curve, and decision curve analysis were conducted using the R packages 'pROC', 'rms', and 'rmda'.

Immune Infiltration Analysis of Psoriasis Subgroup

Patients diagnosed with psoriasis were categorized into two separate groups using the nomoscore, enabling differentiation. Five algorithms (CIBERSORT,[22] ssGSEA,[23] Estimate,[24] MCPcounter,[25] and QuanTIseq[26]) were used to analyze the immune cell composition in psoriasis, aiming to enhance comprehension of the immune microenvironment in high and low-risk groups. To illustrate the results, bar plots, and box plots were utilized to visualize and compare the proportions of each immune cell type between the two groups.

Human Abdominal Aorta and Psoriasis Tissue Specimens

Specimens of human abdominal aortic aneurysm and psoriasis tissue were obtained from patients receiving treatment at the Affiliated Hospital of Chengdu University. Normal abdominal aorta and normal skin tissue were obtained from organ donors. All patients had no tumors, severe infections, or connective tissue diseases. The inclusion of tissue specimens in

this study was approved by the patients themselves or their relatives, and consent forms were signed. The study adhered to the ethical standards outlined in the 1975 Declaration of Helsinki. The study protocol was approved by the institutional review committee of the Affiliated Hospital of Chengdu University (approval No: PJ2023-002-01) and complied with the ethical guidelines of the Office of Research Compliance and Human Research Protection Program.

Western Blotting

Tissues from various experimental groups were harvested and lysed in radioimmunoprecipitation assay buffer supplemented with phosphatase and protease inhibitors (MCE). After quantification of the protein concentrations, the cell lysate or protein samples (20 ug/lane) were separated using Future-PAGE™ on 8% to 12% gels (ACE Biotechnology, Jiangsu, China) and transferred to polyvinylidene difluoride membranes (Millipore, Bedford, MA, USA). The membranes were blocked with protein-free rapid blocking solution (Servicebio Biotechnology, G2052, Wuhan, China) at room temperature for 30 minutes and incubated with primary antibodies overnight at 4°C. The following primary antibodies were used: mouse anti-GAPDH (Proteintech,60004-1-lg, Wuhan, China), rabbit anti-IL7R (Proteintech,17626-1-lg, Wuhan, China); mouse anti-ITGAL (Proteintech,66256-1-lg, Wuhan, China); rabbit anti-HCLS1 (Proteintech,25003-1-lg, Wuhan, China); rabbit anti-GBP5 (Cell Signaling Technologies, 67798, Beverly, MA, USA); rabbit anti-CCR7 (Proteintech,25898-1-lg, Wuhan, China); rabbit anti-CD3D (Proteintech,16669-1-lg, Wuhan, China).

Real-Time Polymerase Chain Reaction

After the collected tissue samples are broken down, subsequent experiments will be conducted Total RNA was extracted from Tissues by using Trizol reagent (Invitrogen, Carlsbad, CA, USA). Each RNA sample was reverse transcribed into cDNA by using the Evo M-MLV RT Kit with gDNA Clean for PCR and applying the SYBR Green Premix Pro Tap HS qPCR Kit (Accurate Biology, Hunan, China). The testing instrument was the Roche Light Cycler 480 Real-Time PCR System (Rocher, Basel, Swiss Confederation). The primer sequences are provided in Supplementary Table 1.

Immunohistochemical (IHC)

We performed immunohistochemical (IHC) analysis to assess the differential expressions of CCR7 (1:100 dilution, Proteintech,55425-1-AP, Wuhan, China); CD3D (1:200 dilution, Proteintech,16669-1-lg, Wuhan, China); GBP5 (1:200 dilution, Proteintech,13220-1-AP, Wuhan, China); HCLS1 (1:200 dilution Proteintech,25003-1-lg, Wuhan, China); IL7R (1:100 dilution, Abcam, ab259806, Cambridge, UK), and ITGAL (1:100 dilution, Proteintech,15574-1-AP, Wuhan, China) in different groups. After antigen retrieval and blocking, the following primary antibodies were diluted in a suitable antibody diluent and applied to the sections, which were then incubated overnight at 4°C. Next, a suitable secondary antibody conjugated with a detection system was applied to the slices. Finally, 3.3′-diaminobenzidine was applied for color development, and the nuclei were counterstained with hematoxylin. The sections were imaged using an optical microscope at 10×–20× magnification.

Statistical Analysis

We performed statistical analysis in our research utilizing the R software (version 4.1.0). Group differences were assessed using either the Wilcoxon test or Student's t-test. GraphPad v9.0 software (San Diego, CA, USA) was used to analyze and make some graphs, Two-sided P values were calculated for all tests, with statistical significance defined as $P < 0.05$.

Results

## Identification and Functional Annotation of Differentially Expressed Genes in Psoriasis

Prior to identifying DEGs, we performed PCA analysis to visualize the distribution of principal components for each group. The PCA plot demonstrated clear differentiation between normal skin and psoriasis samples, as shown in Supplementary Figure 1. By applying a threshold of $|log2FC| \geq 1$ and adjusted $P < 0.05$, we found 575 differentially expressed genes (DEGs) in GSE13355, 1528 DEGs in GSE153007, 313 DEGs in GSE166388, 1718 DEGs in GSE181318, 3075 DEGs in GSE182740, 1680 DEGs in GSE226244, 152 DEGs in GSE63741, 1211 DEGs in GSE6823, 2416 DEGs in GSE78097, and 277 DEGs in GSE79704 (Figure 1A). DEGs that were consistently overlapped in at least two datasets were defined as calibrated differential genes

A
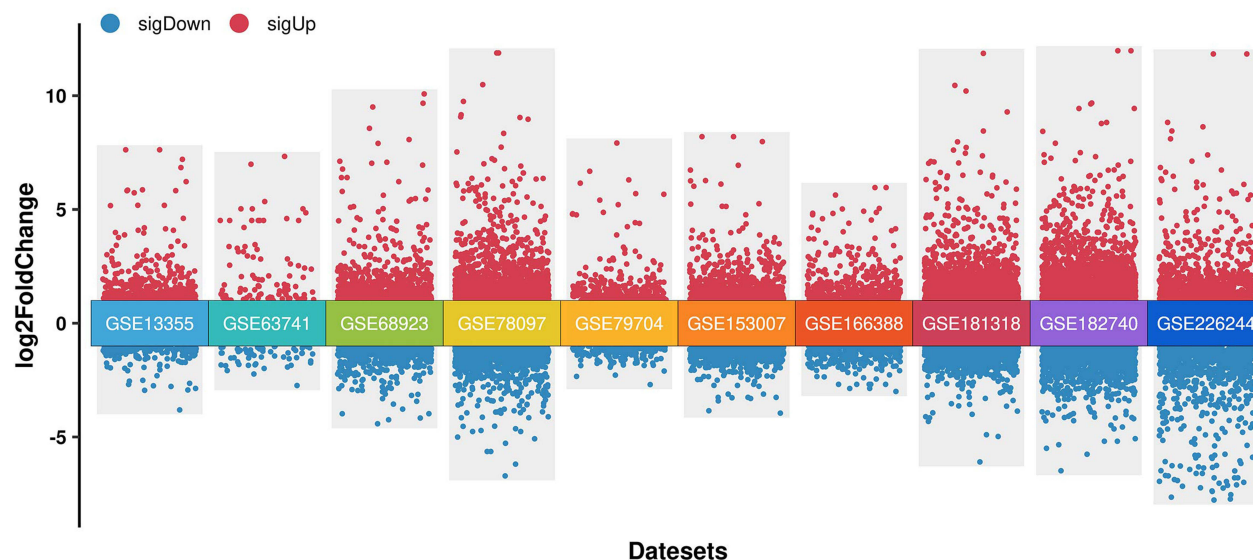
B
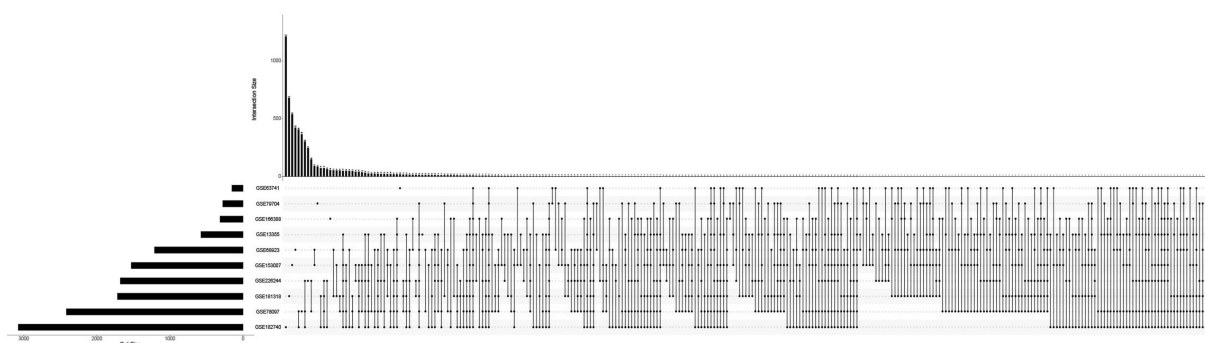
Figure 1 Landscape of DEGs in psoriasis. (**A**) Differential gene expression analysis showing up-and down-regulated genes across ten datasets. An adjusted *P* value < 0.05 and log2FC ≥ 1 is indicated in red, while an adjusted *P* value < 0.05 and log2FC ≤ 1 is indicated in blue. (**B**) Upset diagram showing the intersection across ten datasets.

([Figure 1B](#)). The top 30 enrichment results in terms of biological processes primarily showed cytokine production, immune response, epidermis development, and response to molecules of bacterial origin ([Figure 2A](#)). Concerning molecular function, these DEGs were mainly associated with cytokines, cytokine receptors, peptidase inhibitors, enzyme inhibitors, and steroid binding and activity ([Figure 2B](#)). In terms of cellular components, the intersecting DEGs were predominantly located in the plasma membrane, granule lumen, and vesicle lumen ([Figure 2C](#)). Significant KEGG pathways identified by the GSEA algorithm, where DEGs were mainly enriched, included ligand-receptor interaction such as toll-like receptor signaling pathway, cytokine-cytokine receptor interaction, nod-like receptor signaling pathway, jak stat signaling pathway, t cell receptor signaling pathway, chemokine signaling pathway, and rig I like receptor signaling pathway ([Figure 2D](#)).

Psoriasis-Related Modules and Genes Identification

To identify highly associated genes with psoriasis, we first performed sample clustering using the GSE226244 dataset. Next, the process involved creating a gene network using the R software package called 'WGCNA'. The sample clustering indicated the absence of outliers ([Supplementary Figure 2A](#)). To achieve a scale-free structure and an average connection of zero, we adjusted the soft power to 10 ([Supplementary Figure 2B](#)). Ten gene co-expression modules were created and displayed in a cluster dendrogram ([Figure 3A](#)). Five modules were deemed crucial and chosen for additional examination due to their correlations and significance values: yellow (r = 0.64, P = 5e-6), pink (r = 0.82, P = 4e-11),
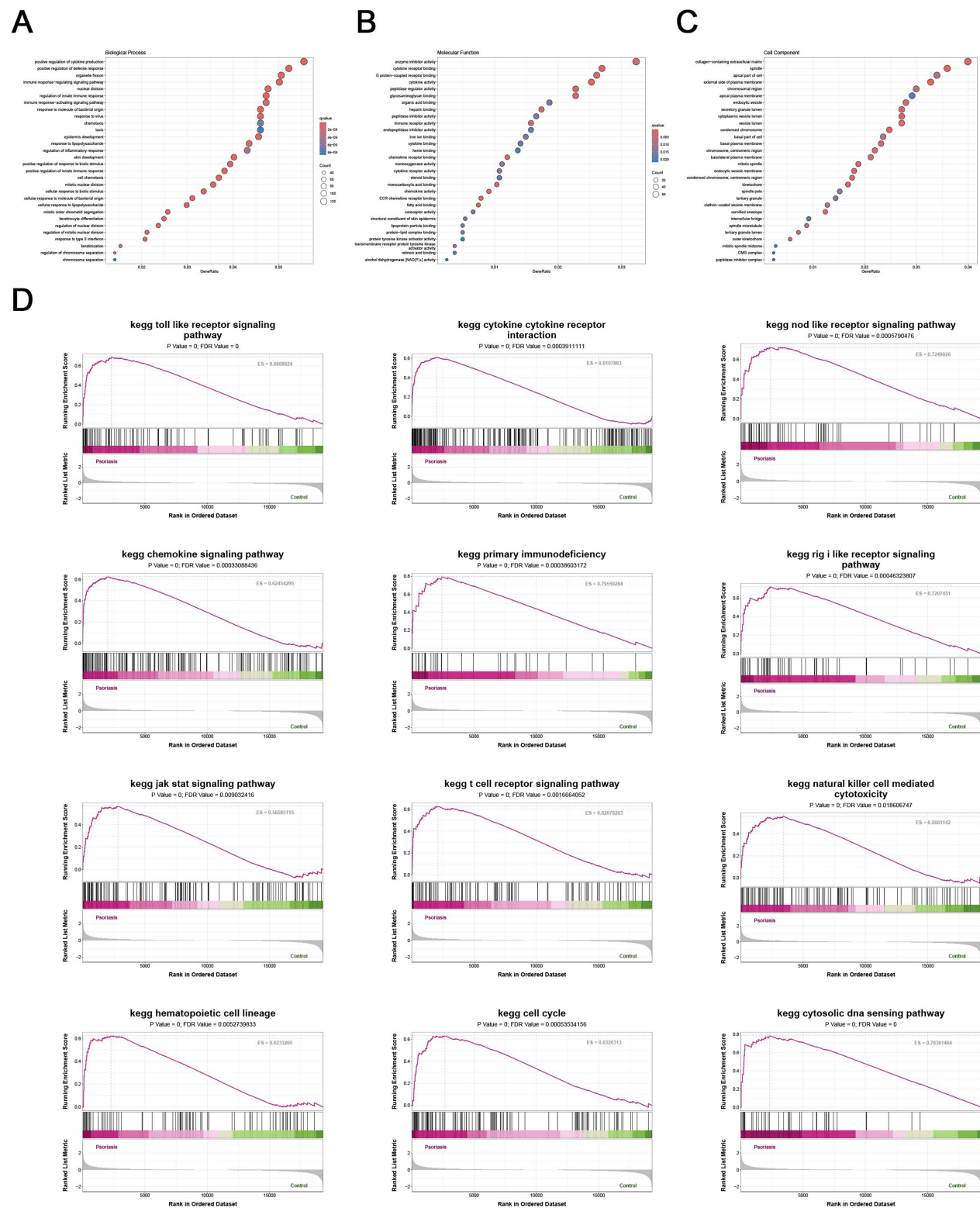
Figure 2 Functional enrichment of DEGs. The top 30 GO enrichment analyses of BP (**A**), MF (**B**), and CC (**C**). The *q* value is scaled by color and gene count is represented by the size of the circle. (**D**) The top 12 KEGG pathway enrichment of GSEA analysis with *P* value < 0.05.
Abbreviations: GO, Gene Ontology. BP, biological process. MF, molecular function. CC, cell component. KEGG, Kyoto Encyclopedia of Genes and Genomes.

turquoise (r = 0.71, P = 2e-7), blue (r = −0.73, P = 6e-8), and green (r = −0.69, P = 5e-7) (Figure 3B). Additionally, we identified the central genes in each group by considering gene importance (GS) greater than 0.2 and module association (MM) greater than 0.8 (Figure 3C). After comparing the differentially expressed genes (DEGs) and hub module genes, we found a total of 1073 shared genes (Figure 3D).

Definition of Core Genes Associated With Abdominal Aortic Aneurysm and Psoriasis

To identify hub genes associated with AAA, we conducted further analysis using the GSE57691 dataset, consisting of 49 AAA and 10 normal aortic artery samples. The samples were distinctly segregated in the two-dimensional principal component distribution (Figure 4A). A total of 1015 DEGs were identified, with 466 showing significant up-regulation and 549 displaying remarkable down-regulation (Figure 4B). By establishing a scale-free topology network with β = 6 (Supplementary Figure 3A), we divided the expression matrix into 20 gene modules (Figure 4C). Among these modules, we identified the tan, black, purple, blue, green, and midnight blue modules as particularly significant (Figure 4D). Subsequently, we identified 176 hub module genes significantly associated with AAA, and then intersected them with the 1015 DEGs of AAA and the 1073 hub genes in psoriasis. Only 20 genes were retained and proceeded to the next step, which involved constructing a risk gene signature (Figure 4E).

Gene Expression Signature Construction

A heatmap was utilized to display the expression patterns of the 20 genes, revealing notably higher expression levels in both psoriasis and AAA (Figure 5A and B). Following this, a network diagram was created by utilizing the STRING database to build a protein-protein interaction (PPI) network (Figure 5C). Friends analysis within the PPI network identified IL7R as a crucial player among these 20 genes (Figure 5D). To identify potential diagnostic indicators for predicting psoriasis patients with AAA, a LASSO regression algorithm identified 6 genes (IL7R, HCLS1, CD3D, ITGAL, CCR7 and GBP5) with minimal logλ = −5.199 (Figure 5E and F). ROC curve analysis showed that the gene signature and most individual genes were highly accurate in diagnosing and predicting psoriasis, as seen in Figure 5G and H. Furthermore, an individualized nomogram for predicting disease risk was successfully constructed, with the relative expression of each gene represented as a score (Figure 5I).

Validation of the Gene Signature and Immune Infiltration of Subgroups

ROC curves were created in three separate testing datasets (GSE79704, GSE13355, and GSE63741) to assess the gene signature's diagnostic precision in psoriasis. The gene signature consistently demonstrated satisfactory accuracy in diagnosing psoriasis across all three validation datasets (0.917 for GSE79704, 0.988 for GSE13355, and 0.798 for GSE63741) (Figure 6A–C). To delve deeper into the accuracy of the gene signature for AAA diagnosis, we conducted thorough evaluations such as ROC curves, decision curve analysis, calibration curve, and precision-recall curve. The results of both GSE57691 and GSE47472 demonstrated that this gene signature exhibited great suitability in assessing the risk of AAA in psoriasis patients (Figure 6D–K).

To explore differences in immune characteristics between subgroups, we utilized five algorithms: CIBERSORT, Estimate, ssGSEA, MCPcounter, and QuanTIseq. The CIBERSORT algorithm indicated that T cells CD4 memory activated and neutrophils were relatively higher in the high-risk subgroup (Figure 6L, Supplementary Figure 3A). Based on the Estimate algorithm, the high-risk subgroup showed elevated Immune Score and ESTIMATE Score (Supplementary Figure 3B). Furthermore, the ssGSEA analysis indicated that aDCs, cytotoxic lymphocytes, iDCs, T lymphocytes, and Th1 lymphocytes were prevalent in the high-risk category (Supplementary Figure 3C). In addition, the MCPcounter analysis revealed an increase in monocytic lineage and myeloid dendritic cells in the high-risk subgroup, whereas the QuanTIseq algorithm showed elevated levels of macrophage M1 and M2 in this subgroup (Supplementary Figure 3D and E). The findings indicate that individuals in the high-risk category showed a heightened immune environment.

Psoriasis and Abdominal Aortic Aneurysm Exhibit Co-Expressed Relevant Genes

After extracting protein and tissue RNA from normal skin tissue, psoriatic tissue, normal abdominal aorta, and abdominal aortic aneurysm tissue, we conducted Western blotting and RT-qPCR experiments. We found that IL7R, HCLS1, CD3D, ITGAL, CCR7, and GBP5 were all significantly upregulated in the disease groups compared to the normal groups. This suggests that these six genes are pathogenic risk genes in both psoriasis and abdominal aortic aneurysm (Figure 7A–C).
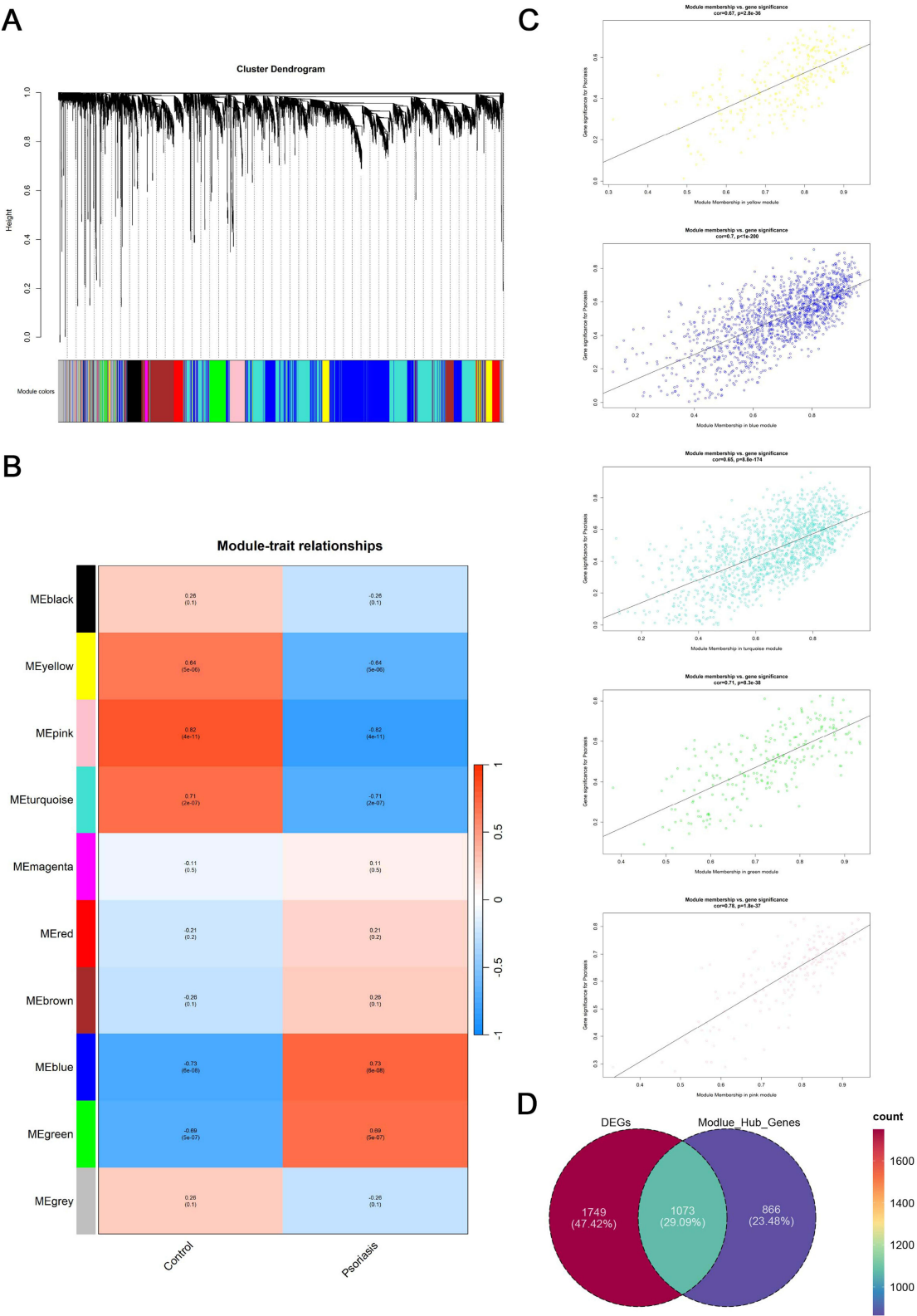
Figure 3 Identification of hub genes in psoriasis. (**A**) The cluster dendrogram of gene modules in psoriasis samples. (**B**) The correlation heatmap indicates module-trait relationships. The first-row number in each block indicates the correlation coefficient, which is scaled by color. The number in parentheses represents the *P* value. (**C**) Scatter diagram of yellow, pink, turquoise, blue, and green modules. The x-axis represents module membership in each module, and the y-axis represents gene significance for psoriasis. (**D**) Venn diagram indicates the intersecting gene between DEGs and module hub genes in psoriasis. Gene count is scaled by color. Gene percentages are displayed below the gene count.
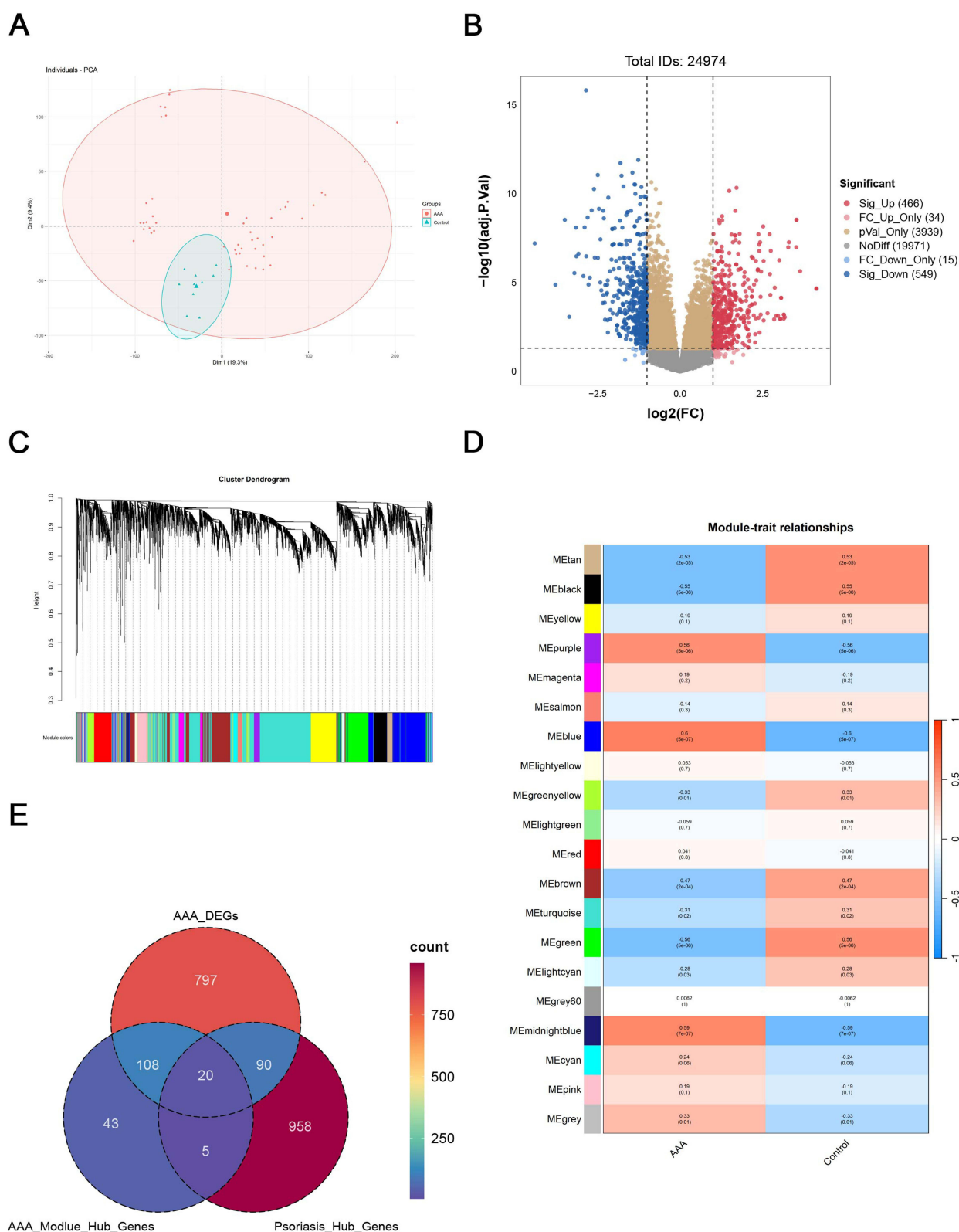
Figure 4 Identification of hub genes between psoriasis and AAA. (**A**) PCA diagram visualizes the two-dimensional distribution of the principal component of AAA and control samples. (**B**) The volcano plot of GSE57693 indicates the distribution of DEGs. AAA, abdominal aortic aneurysm. Control, normal aortic arteries. Genes in red represent significantly up-regulated, blue represents significantly down-regulated, brown represents P value < 0.05, gray represents no significance, light red represents log2FC ≥ 1, and light blue represents log2FC ≤ 1. (**C**) The cluster dendrogram of gene modules in AAA samples. (**D**) The correlation heatmap indicates module-trait relationships. The first-row number in each block indicates the correlation coefficient, which is scaled by color. The number in parentheses represents the *P* value. (**E**) Venn diagram indicates the intersecting gene among DEGs in AAA, module hub genes in AAA, and hub genes in psoriasis. Gene count is scaled by color.
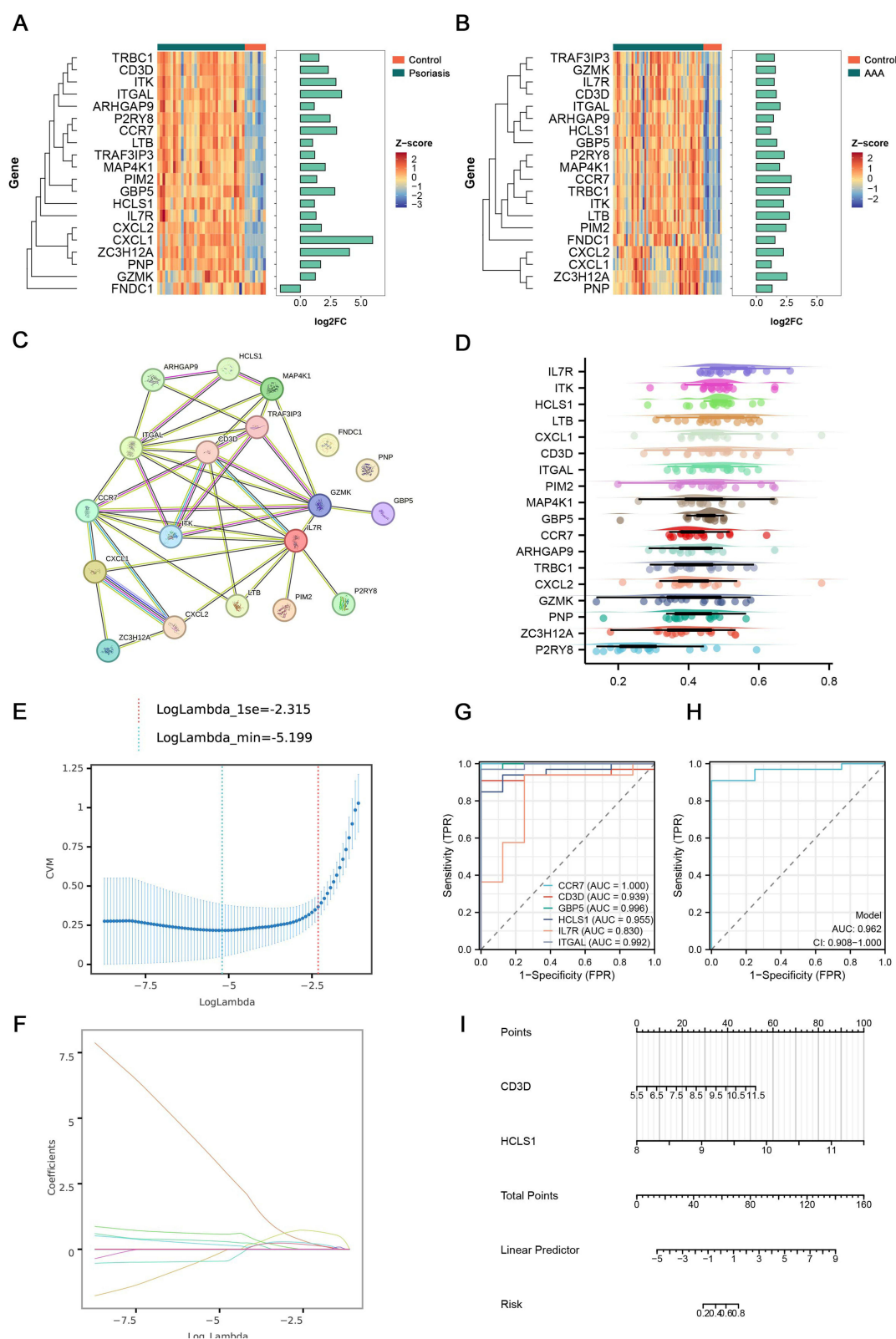
Figure 5 Establishment of gene signature by LASSO regression. (**A** and **B**) Heatmap of 20 hub genes in GSE226244 (**A**) and GSE57691 (**B**). Gene expression is scaled by the Z-score. The bar plot beside the heatmap reveals the log2FC of genes. (**C**) The PPI network constructed by STRING reveals the interaction between these 20 genes. (**D**) Friend analysis discovers the rank of 20 genes. The x-axis indicates the gene similarity. The y-axis represents genes. (**E**) The log (lambda) sequence was used to construct a coefficient profile diagram. (**F**) LASSO coefficient profiles of the 20 genes in psoriasis. (**G** and **H**) ROC curve of CCR7, CD3D, GBP5, HCLS1, IL7R, ITGAL, and the gene signature. (**I**) The visible nomogram for diagnosing psoriasis.

Abbreviations: LASSO, least absolute shrinkage, and selection operator. AUC: area under the curve. CI: 95% confidence interval.
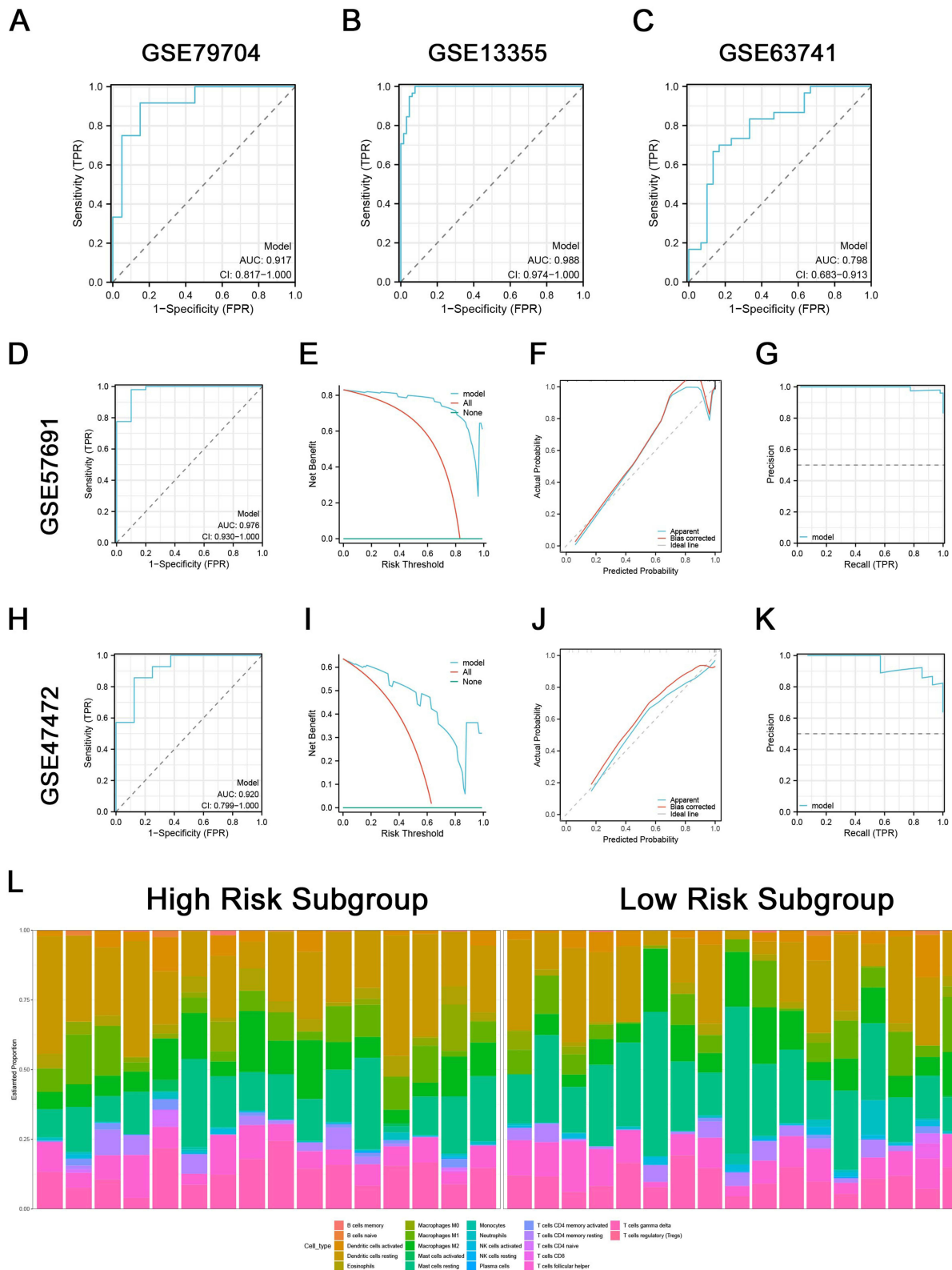
Figure 6 Diagnostic value evaluation of gene signature. (**A–C**) The ROC curves of testing sets (GSE79704, GSE13355, and GSE63741) demonstrate satisfactory accuracy of gene signature predicting psoriasis. (**D**) Robust accuracy of gene signature in predicting AAA risk emerges in the training set (GSE57691) and testing set (GSE47472), followed by ROC curves (**D** and **H**), DCA curves (**E** and **I**), calibration curves (**F** and **J**) and PR curves (**G** and **K**). AUC: area under the curve. CI: 95% confidence interval. (**L**) Histogram indicates the differential immune infiltration of GSE226244 between high-risk and low-risk subgroups. The y-axis represents the percentage of immune cells.
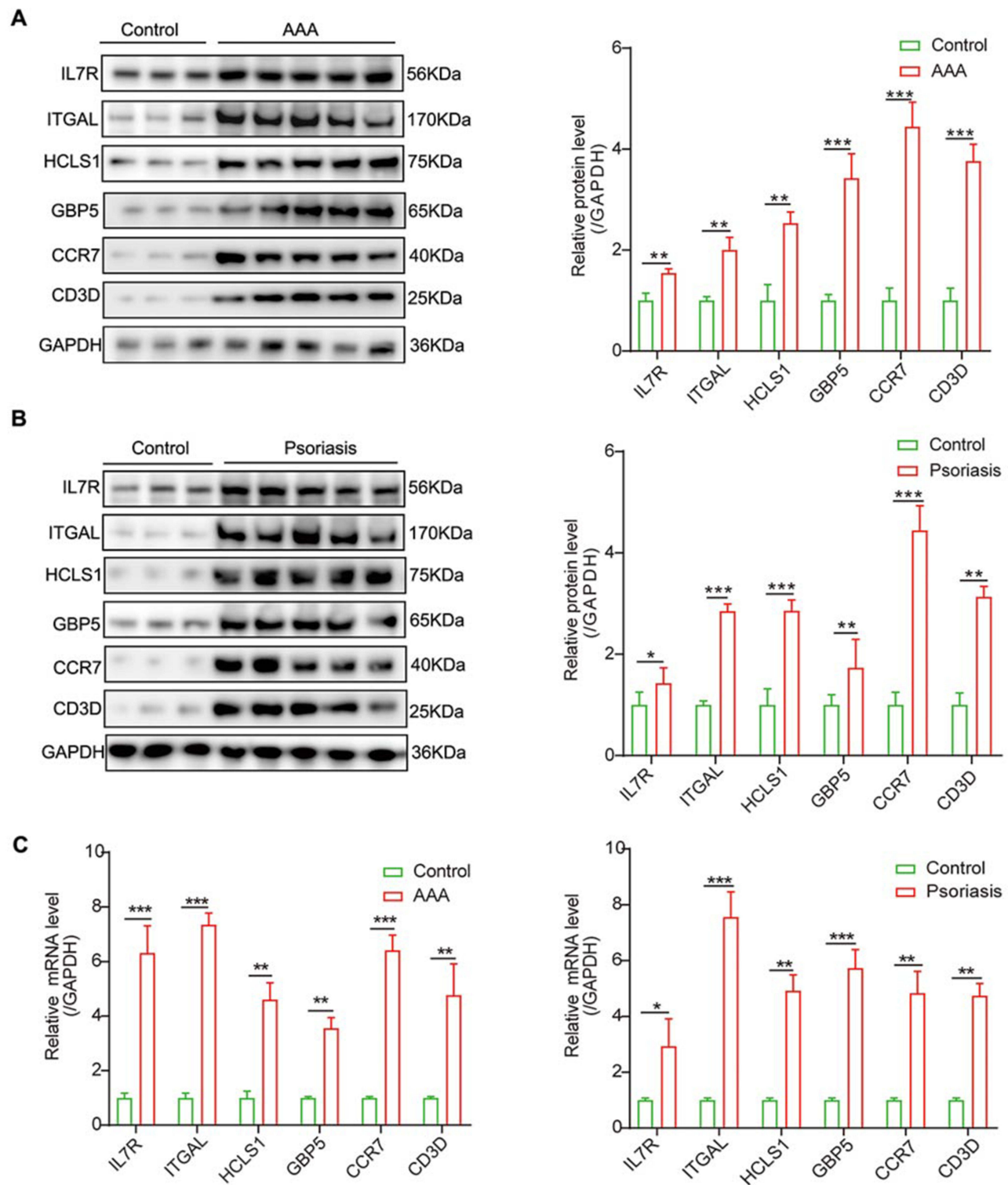
Figure 7 Investigation of candidate gene expression across diverse tissue types. (**A**) Protein extraction from normal abdominal aorta (n=3) and abdominal aortic aneurysm specimens (n=5), followed by Western blot analysis. (**B**) Protein extraction from normal skin tissue (n=3) and psoriatic plaque specimens, followed by Western blot analysis (n=5). (**C**) Utilizing RT-qPCR experiments to analyze RNA extracted from normal abdominal aorta (n=3), abdominal aortic aneurysm (n=5); normal skin (n=3), and psoriatic plaque tissues (n=5).
Note: Data are presented as mean ± SEM (*$p < 0.05$, **$p < 0.01$, ***$p < 0.001$).
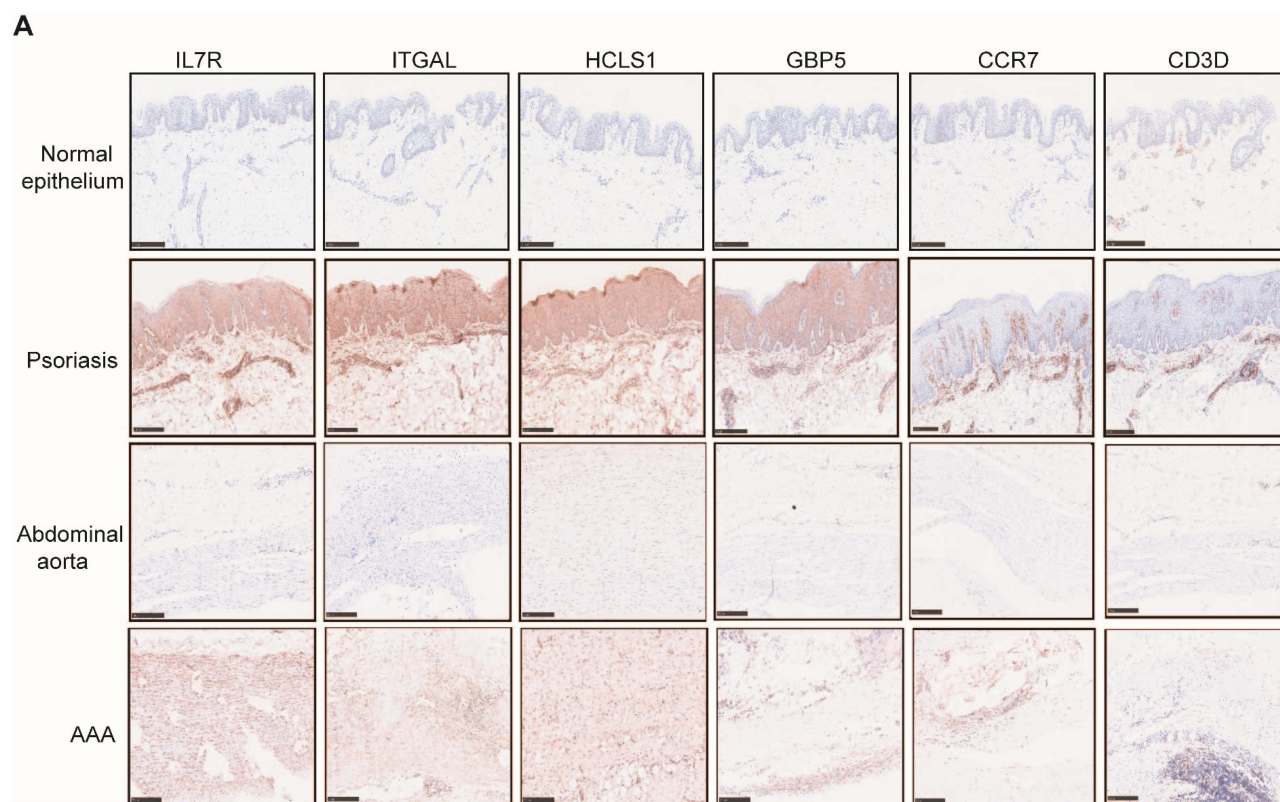
Figure 8 Analysis of gene expression in different tissues. (**A**) Perform immunohistochemical staining on normal abdominal aorta, abdominal aortic aneurysm, normal skin, and psoriatic plaque tissues to observe the expression differences of six candidate genes (scale bars: IHC, 250μm; n = 3 per group).

By conducting immunohistochemical staining on tissues from normal and diseased groups, we observed higher expression of the six genes in psoriatic tissue compared to normal skin tissue, and a similar trend was noted in abdominal aortic aneurysm tissue compared to normal aortic tissue (Figure 8A).

Discussion

Emerging research highlights that psoriasis is not merely a skin condition but a systemic disease linked with various comorbidities, such as cardiovascular diseases.[27–30] Prioritizing early interventions and treatments that address both the disease and its associated conditions is essential. Recent insights reveal that psoriasis operates under the influence of intricate interactions between cytokines outside the cell and signal molecules within.[31] These cytokines deliver signals to receptors on the cell membrane, initiating a series of intracellular events that precipitate inflammatory cascades.[32,33] Such cascades not only exacerbate psoriasis but also lead to several comorbidities, including AAA.[6] Research identifies AAA as a notable comorbidity, stemming from shared genetic factors, enhanced oxidative stress, and similar inflammatory processes seen in psoriasis.[34–36] Specifically, the TNF-IL-23-IL-17 axis, crucial in psoriasis pathogenesis, has also been implicated in AAA development. Increased levels of IL-17 and IL-23 have been documented in the aortic tissues of AAA patients relative to controls. The role of IL-17, produced by CD4$^+$ T cells, encompasses the modulation of inflammation, apoptosis in aortic SMCs, and vascular remodeling.[37] Additionally, TNF-α, predominantly expressed in psoriatic lesions, contributes to AAA through the activation of MMP-2 and MMP-9. These enzymes are involved in the degradation of elastic fibers, facilitating aneurysm growth.[38] Identifying these molecular targets is crucial for assessing AAA risks in psoriasis patients and enhancing the efficacy of treatments for AAA in the context of psoriasis.

In this study, we identified six pivotal genes implicated in the progression of both psoriasis and AAA. These genes serve as effective predictors for assessing the risk of AAA development in patients with psoriasis. Chemokines regulate immune cell migration during inflammation and play a key role in chronic inflammatory diseases.[39] CCR7 facilitates

interactions among dendritic cells and various T cell subsets, affecting immune responses in states like inflammation, tolerance, and autoimmunity.[40] Studies have shown that psoriasis patients have higher levels of CCR7^{+} T lymphocytes compared to healthy controls, contributing to persistent inflammatory states.[41] Additionally, CCR7 and its ligands promote the formation of tertiary lymphoid organs (TLOs), which are implicated in chronic inflammation in psoriasis and can exacerbate disease progression.[42] In the vascular context, CCR7 may enhance interactions between stromal cells and immune cells, fostering the formation of tertiary lymphoid organs (TLOs). This activity not only influences inflammatory processes in the aneurysm wall but also contributes to the development and progression of AAA.[43] Our findings suggest that CCR7 serves as a significant predictor for AAA risk in psoriasis patients, indicating its dual role in these diseases and its potential as a target for therapeutic intervention.

IL-7 and its receptor, IL-7R, are crucial for T and B cell development in mice, facilitating naive T cell differentiation and memory T cell maintenance.[44] They also play a central role in developing and sustaining innate lymphoid cells (ILCs), which are vital for lymphoid architecture and protective barriers.[45] Studies highlight IL-7R's significant role in the interconnected pathogenesis of psoriasis and depression, particularly through its regulation of T-cell activities.[46] Additionally, IL-7R is instrumental in sustaining type 2 innate lymphoid cell (ILC2) functionality, indirectly influencing AAA progression via IL-5 and eosinophils.[47] Our research links elevated IL-7R expression in psoriasis patients to a heightened risk of AAA, underscoring IL-7R's critical role in both conditions. Further experiments are needed to elucidate IL-7R's specific mechanisms in these both diseases.

HCLS1, also known as HS1, critically regulates actin dynamics at the T-cell immunological synapse and impacts various natural killer (NK) cell functions such as chemotaxis, cell adhesion, and actin assembly during cell lysis.[48] Furthermore, HCLS1's involvement in leukemic B cell migration, trafficking, and homing underscores its significant influence on leukemia progression.[49] Within the context of peripheral vascular atherosclerosis (PVA), HCLS1 has been identified as a key gene associated significantly with the condition. Preliminary analyses suggest HCLS1's potential role in modulating immune responses and vascular functions, which are vital in PVA's pathogenesis.[50] While the specific contributions of HCLS1 to psoriasis and AAA remain underexplored, our analysis suggests that HCLS1 could act as a predictive marker for AAA risk among psoriasis patients, potentially via mechanisms related to T cell activity. This hypothesis is supported by significant differences in certain T cell types between high and low-risk groups based on immune infiltration scores. Further research is necessary to elucidate these associations.

CD3D, a component of the T-cell receptor/CD3 complex crucial for T-cell activation, is downregulated in psoriasis patients responding favorably to alefacept therapy.[51,52] This suggests that modulation of CD3D expression could serve as a potential marker to distinguish responders from non-responders to alefacept treatment, highlighting its role in regulating T-cell activity and its potential as a therapeutic target in inflammatory diseases.[53] However, research on CD3D in vascular diseases is lacking. Given the known involvement of T cells in the pathogenesis of AAA,[54] our findings of significant differences in certain T-cell types between high and low-risk groups underscore the potential of CD3D as a critical target for predicting and potentially treating AAA in psoriasis patients.

Leukocytes are key in psoriasis and AAA diseases.[55,56] ITGAL, or CD11A, encodes the alpha L chain of integrins, heterodimeric proteins with alpha and beta chains. This alpha integrin forms LFA-1 with the beta 2 chain (ITGB2), crucial for leukocyte adhesion and costimulatory signaling through its ligands, ICAMs.1−3 [57] LFA-1 is essential in immune responses, mediating interactions between leukocytes and endothelial cells. Efalizumab, a recombinant humanized monoclonal antibody targeting CD11A, the alpha subunit of LFA-1, is approved for treating adults with chronic moderate-to-severe plaque psoriasis.[58] Additionally, CD11A facilitates the penetration of neutrophils through the vascular endothelium, crucial for maintaining endothelial integrity and function, and is linked to inflammatory infiltration and extracellular matrix degradation in AAA pathogenesis.[59] Exploring the potential roles of ITGAL in psoriasis and AAA may provide insights into the mechanisms underlying these diseases and offer theoretical foundations for new therapeutic approaches.

Recently, interferons have been recognized as key mediators in the pathogenesis of psoriasis. Type I interferons, crucial cytokines associated with chronic viral infections, often trigger psoriasis and psoriatic arthritis when used therapeutically.[60] GBP5, a member of the TRAFAC class dynamin-like GTPase superfamily, plays a role in antiviral mechanisms through IFN-stimulated gene pathways and cytokine signaling in the immune system.[61] Furthermore, GBP5-

encoded proteins act as activators in the assembly of the NLRP3 inflammasome, impacting innate immunity and inflammation.[62] Studies suggest that inhibiting the NLRP3 inflammasome through lysosome-dependent pathways can reduce inflammation and slow the progression of AAA.[63] Our immune infiltration analysis indicates significant alterations in macrophages in psoriasis patients. Changes in these NLRP3-related macrophages may underlie the potential mechanism linking psoriasis to the development of AAA.

In further basic experiments, we found high expression of the six genes in both psoriatic tissue and abdominal aortic aneurysm tissue, further confirming the conclusions drawn from bioinformatic analysis. This suggests a potential association between psoriasis patients and the risk of developing abdominal aortic aneurysm. However, although we identified risk genes in this experiment, we did not further validate them at the mechanistic level, which is a limitation of this study. This will be addressed in subsequent experiments.

Conclusion

In summary, this study utilized public datasets on psoriasis and AAA to uncover a gene signature comprising six risk genes, innovatively structured to reveal shared pathogenetic links and regulatory mechanisms between these conditions. Furthermore, it detailed the immune infiltration landscape that predicts a higher risk of AAA in patients with psoriasis. These insights provide crucial theoretical targets for the diagnosis and treatment of AAA development in psoriasis patients.

Abbreviations

AAA, Abdominal aortic aneurysm; WGCNA, Weighted gene correlation network analysis; GEO, Gene Expression Omnibus; DEGs, Differentially expressed genes; MM, Module membership; GS, Gene significance; GO, Gene Ontology; KEGG, Kyoto Encyclopedia of Genes and Genomes; GSEA, Gene set enrichment analysis; PPI, Protein-protein interaction.

Data Sharing Statement

The datasets GSE226244, GSE182740, GSE181318, GSE166388, GSE153007, GSE68923 (containing GSE68937), GSE78097, GSE79074, GSE63741, GSE13355, GSE57691 and GSE47472 for this study can be found in the online repositories. (https://www.ncbi.nlm.nih.gov/).

Ethics Declaration

The studies involving human participants were reviewed and approved by the Institutional Ethics Committee for Clinical Research of the Affiliated Hospital of Chengdu University (approval No: PJ2023-002-01) and complied with the ethical guidelines of the Office of Research Compliance and Human Research Protection Program. The patients/participants provided their written informed consent to participate in this study. Conscious donors all personally signed written consent forms; for some critically ill or even in shock abdominal aortic aneurysm patients, consent forms were signed by their family members.

Author Contributions

The authors declare that all authors made a significant contribution to the work reported, whether that is in the conception, study design, execution, acquisition of data, analysis and interpretation, or in all these areas; took part in drafting, revising or critically reviewing the article; gave final approval of the version to be published; have agreed on the journal to which the article has been submitted; and agree to be accountable for all aspects of the work.

Funding

Disclosure

The authors report no conflicts of interest in this work.

References

1. Dey AK, Joshi AA, Chaturvedi A, et al. Association between skin and aortic vascular inflammation in patients with psoriasis: a case-cohort study using positron emission tomography/computed tomography. *JAMA Cardiol*. 2017;2(9):1013–1018. doi:10.1001/jamacardio.2017.1213

2. Gelfand JM, Neimann AL, Shin DB, Wang X, Margolis DJ, Troxel AB. Risk of myocardial infarction in patients with psoriasis. *JAMA*. 2006;296 (14):1735–1741. doi:10.1001/jama.296.14.1735

3. Khalid U, Ahlehoff O, Gislason GH, et al. Psoriasis and risk of heart failure: a nationwide cohort study. *Eur J Heart Fail*. 2014;16(7):743–748. doi:10.1002/ejhf.113

4. Samarasekera EJ, Neilson JM, Warren RB, Parnham J, Smith CH. Incidence of cardiovascular disease in individuals with psoriasis: a systematic review and meta-analysis. *J Invest Dermatol*. 2013;133(10):2340–2346. doi:10.1038/jid.2013.149

5. Golledge J. Abdominal aortic aneurysm: update on pathogenesis and medical treatments. *Nat Rev Cardiol Apr*. 2019;16(4):225–242. doi:10.1038/s41569-018-0114-9

6. Libby P. The molecular mechanisms of the thrombotic complications of atherosclerosis. *J Intern Med*. 2008;263(5):517–527. doi:10.1111/j.1365-2796.2008.01965.x

7. Naik HB, Natarajan B, Stansky E, et al. Severity of psoriasis associates with aortic vascular inflammation detected by FDG PET/CT and neutrophil activation in a prospective observational study. *Arterioscler Thromb Vasc Biol*. 2015;35(12):2667–2676. doi:10.1161/atvbaha.115.306460

8. Chiu HY, Lo PC, Huang WF, Tsai YW, Tsai TF. Increased risk of aortic aneurysm (AA) in relation to the severity of psoriasis: a national population-based matched-cohort study. *J Am Acad Dermatol*. 2016;75(4):747–754. doi:10.1016/j.jaad.2016.06.002

9. Khalid U, Egeberg A, Ahlehoff O, Smedegaard L, Gislason GH, Hansen PR. Nationwide study on the risk of abdominal aortic aneurysms in patients with psoriasis. *Arterioscler Thromb Vasc Biol*. 2016;36(5):1043–1048. doi:10.1161/atvbaha.116.307449

10. No DJ, Amin M, Duan L, Egeberg A, Ahlehoff O, Wu JJ. Risk of aortic aneurysm in patients with psoriasis: a retrospective cohort study. *J Eur Acad Dermatol Venereol*. 2018;32(2):e54–e56. doi:10.1111/jdv.14496

11. Yu X, Feng X, Xia L, Cao S, Wei X. Risk of aortic aneurysm in patients with psoriasis: a systematic review and meta-analysis of cohort studies. *Clin Cardiol*. 2020;43(11):1266–1272. doi:10.1002/clc.23438

12. Armstrong AW, Pathophysiology RC. Clinical presentation, and treatment of psoriasis: a review. *JAMA*. 2020;323(19):1945–1960. doi:10.1001/jama.2020.4006

13. Guo J, Zhang H, Lin W, Lu L, Su J, Chen X. Signaling pathways and targeted therapies for psoriasis. *Signal Transduct Target Ther*. 2023;8(1):437. doi:10.1038/s41392-023-01655-6

14. Marquez-Sanchez AC, Koltsova EK. Immune and inflammatory mechanisms of abdominal aortic aneurysm. *Front Immunol*. 2022;13:989933. doi:10.3389/fimmu.2022.989933

15. Srivastava AK, Chand Yadav T, Khera HK, et al. Insights into interplay of immunopathophysiological events and molecular mechanistic cascades in psoriasis and its associated comorbidities. *J Autoimmun*. 2021;118:102614. doi:10.1016/j.jaut.2021.102614

16. Langfelder P, Horvath S. WGCNA: an R package for weighted correlation network analysis. *BMC Bioinf*. 2008;9:559. doi:10.1186/1471-2105-9-559

17. The gene ontology resource: 20 years and still GOing strong. *Nucleic Acids Res*. 2019;47(D1):D330–d338. doi:10.1093/nar/gky1055

18. Yu G, Wang L-G, Han Y, He Q-Y. clusterProfiler: an R package for comparing biological themes among gene clusters. *OMICS*. 2012;16 (5):284–287. doi:10.1089/omi.2011.0118

19. Subramanian A, Tamayo P, Mootha VK, et al. Gene set enrichment analysis: a knowledge-based approach for interpreting genome-wide expression profiles. *Proc Natl Acad Sci USA*. 2005;102(43):15545–15550. doi:10.1073/pnas.0506580102

20. Friedman J, Hastie T, Tibshirani R. Regularization paths for generalized linear models via coordinate descent. *Journal of Statistical Software*. 2010;33(1):1–22. doi:10.18637/jss.v033.i01

21. Chen S, Liu S, Xu S, et al. Naples prognostic score is an independent prognostic factor in patients with small cell lung cancer and nomogram predictive model established. *J Inflamm Res*. 2022;15:3719–3731. doi:10.2147/jir.S371545

22. Newman AM, Liu CL, Green MR, et al. Robust enumeration of cell subsets from tissue expression profiles. *Nature Methods*. 2015;12(5):453–457. doi:10.1038/nmeth.3337

23. Barbie DA, Tamayo P, Boehm JS, et al. Systematic RNA interference reveals that oncogenic KRAS-driven cancers require TBK1. *Nature*. 2009;462(7269):108–112. doi:10.1038/nature08460

24. Yoshihara K, Shahmoradgoli M, Martínez E, et al. Inferring tumour purity and stromal and immune cell admixture from expression data. *Nat Commun*. 2013;4:2612. doi:10.1038/ncomms3612

25. Becht E, Giraldo NA, Lacroix L, et al. Estimating the population abundance of tissue-infiltrating immune and stromal cell populations using gene expression. *Genome Biol*. 2016;17(1):218. doi:10.1186/s13059-016-1070-5

26. Finotello F, Mayer C, Plattner C, et al. Molecular and pharmacological modulators of the tumor immune contexture revealed by deconvolution of RNA-seq data. *Genome Med*. 2019;11(1):34. doi:10.1186/s13073-019-0638-6

27. Takeshita J, Grewal S, Langan SM, et al. Psoriasis and comorbid diseases: implications for management. *J Am Acad Dermatol*. 2017;76 (3):393–403. doi:10.1016/j.jaad.2016.07.065

28. Korman NJ. Management of psoriasis as a systemic disease: what is the evidence? *Br J Dermatol*. 2020;182(4):840–848. doi:10.1111/bjd.18245

29. Kõks S, Kingo K, Vabrit K, et al. Possible relations between the polymorphisms of the cytokines IL-19, IL-20 and IL-24 and plaque-type psoriasis. *Genes Immun*. 2005;6(5):407–415. doi:10.1038/sj.gene.6364216

30. Kingo K, Kõks S, Nikopensius T, Silm H, Vasar E. Polymorphisms in the interleukin-20 gene: relationships to plaque-type psoriasis. *Genes Immun*. 2004;5(2):117–121. doi:10.1038/sj.gene.6364046

31. Uppala R, Tsoi LC, Harms PW, et al. "Autoinflammatory psoriasis"-genetics and biology of pustular psoriasis. *Cell mol Immunol*. 2021;18 (2):307–317. doi:10.1038/s41423-020-0519-3

32. Kõks G, Uudelepp ML, Limbach M, Peterson P, Reimann E, Kõks S. Smoking-induced expression of the GPR15 gene indicates its potential role in chronic inflammatory pathologies. *Am J Pathol*. 2015;185(11):2898–2906. doi:10.1016/j.ajpath.2015.07.006

33. Kõks S, Kõks G. Activation of GPR15 and its involvement in the biological effects of smoking. *Exp Biol Med*. 2017;242(11):1207–1212. doi:10.1177/1535370217703977

34. Lu S, White JV, Nwaneshiudu I, et al. Human abdominal aortic aneurysm (AAA): evidence for an autoimmune antigen-driven disease. *Autoimmun Rev*. 2022;21(10):103164. doi:10.1016/j.autrev.2022.103164

35. Golledge J, Thanigaimani S, Powell JT, Tsao PS. Pathogenesis and management of abdominal aortic aneurysm. *Eur Heart J*. 2023;44 (29):2682–2697. doi:10.1093/eurheartj/ehad386

36. Griffiths CE, Barker JN. Pathogenesis and clinical features of psoriasis. *Lancet*. 370:9583):263–271. doi:10.1016/S0140-6736(07)61128-3

37. Sharma AK, Lu G, Jester A, et al. Experimental abdominal aortic aneurysm formation is mediated by IL-17 and attenuated by mesenchymal stem cell treatment. *Circulation*. 2012;126(11 Suppl 1):S38–45. doi:10.1161/CIRCULATIONAHA.111.083451

38. Kurashiki T, Miyake T, Nakagami H, Nishimura M, Morishita R. Prevention of progression of aortic aneurysm by peptide vaccine against ang ii (angiotensin ii) in a rat model. *Hypertension*. 2020;76(6):1879–1888. doi:10.1161/HYPERTENSIONAHA.119.14442

39. Griffith JW, Sokol CL, Luster AD. Chemokines and chemokine receptors: positioning cells for host defense and immunity. *Annu Rev Immunol*. 2014;32:659–702. doi:10.1146/annurev-immunol-032713-120145

40. Luther SA, Bidgol A, Hargreaves DC, et al. Differing activities of homeostatic chemokines CCL19, CCL21, and CXCL12 in lymphocyte and dendritic cell recruitment and lymphoid neogenesis. *J Immunol*. 2002;169(1):424–433. doi:10.4049/jimmunol.169.1.424

41. Bose F, Petti L, Diani M, et al. Inhibition of CCR7/CCL19 axis in lesional skin is a critical event for clinical remission induced by TNF blockade in patients with psoriasis. *Am J Pathol*. 2013;183(2):413–421. doi:10.1016/j.ajpath.2013.04.021

42. Brandum EP, Jorgensen AS, Rosenkilde MM, Hjorto GM. Dendritic cells and ccr7 expression: an important factor for autoimmune diseases, chronic inflammation, and cancer. *Int J mol Sci*. 2021;22(15). doi:10.3390/ijms22158340

43. Sun X, Lu Y, Wu J, et al. Meta-analysis of single-cell RNA-seq data reveals the mechanism of formation and heterogeneity of tertiary lymphoid organ in vascular disease. *Arterioscler Thromb Vasc Biol*. 2023;43(10):1867–1886. doi:10.1161/ATVBAHA.123.318762

44. Barata JT, Durum SK, Seddon B. Flip the coin: IL-7 and IL-7R in health and disease. *Nat Immunol*. 2019;20(12):1584–1593. doi:10.1038/s41590-019-0479-x

45. Willis CR, Seamons A, Maxwell J, et al. Interleukin-7 receptor blockade suppresses adaptive and innate inflammatory responses in experimental colitis. *J Inflamm*. 2012;9(1):39. doi:10.1186/1476-9255-9-39

46. Xia X, Yu H, Li Y, Liang Y, Li G, Huang F. Transcriptome analysis identifies biomarkers for the diagnosis and management of psoriasis complicated with depression. *Clin Cosmet Invest Dermatol*. 2023;16:1287–1301. doi:10.2147/CCID.S413887

47. Zhang Y, Liu T, Deng Z, et al. Group 2 innate lymphoid cells protect mice from abdominal aortic aneurysm formation via Il5 and eosinophils. *Adv Sci*. 2023;10(7):e2206958. doi:10.1002/advs.202206958

48. Castro-Ochoa KF, Guerrero-Fonseca IM, Schnoor M. Hematopoietic cell-specific lyn substrate (HCLS1 or HS1): a versatile actin-binding protein in leukocytes. *J Leukoc Biol*. 2019;105(5):881–890. doi:10.1002/JLB.MR0618-212R

49. Scielzo C, Bertilaccio MT, Simonetti G, et al. HS1 has a central role in the trafficking and homing of leukemic B cells. *Blood*. 2010;116 (18):3537–3546. doi:10.1182/blood-2009-12-258814

50. Xie W, Chen S, Luo H, Kong C, Wang D. Critical gene signature and immunological characterization in peripheral vascular atherosclerosis: novel insights from Mendelian randomization and transcriptomics. *Front Genet*. 2024;15:1361445. doi:10.3389/fgene.2024.1361445

51. Haider AS, Lowes MA, Gardner H, et al. Novel insight into the agonistic mechanism of alefacept in vivo: differentially expressed genes may serve as biomarkers of response in psoriasis patients. *J Immunol*. 2007;178(11):7442–7449. doi:10.4049/jimmunol.178.11.7442

52. Ma D, Zhong S, Liu X, et al. CD3D and PRKCQ work together to discriminate between B-cell and T-cell acute lymphoblastic leukemia. *Comput Biol Med*. 2016;77:16–22. doi:10.1016/j.compbiomed.2016.07.004

53. Gil J, Busto EM, Garcillan B, et al. A leaky mutation in CD3D differentially affects alphabeta and gammadelta T cells and leads to a Talphabeta-Tgammadelta+B+NK+ human SCID. *J Clin Invest*. 2011;121(10):3872–3876. doi:10.1172/JCI44254

54. Yuan Z, Lu Y, Wei J, Wu J, Yang J, Cai Z. Abdominal aortic aneurysm: roles of inflammatory cells. *Front Immunol*. 2020;11:609161. doi:10.3389/fimmu.2020.609161

55. Liu YJ, Li R, Xiao D, et al. Incorporating machine learning and PPI networks to identify mitochondrial fission-related immune markers in abdominal aortic aneurysms. *Heliyon*. 2024;10(7):e27989. doi:10.1016/j.heliyon.2024.e27989

56. Johnson-Huang LM, Pensabene CA, Shah KR, et al. Post-therapeutic relapse of psoriasis after CD11a blockade is associated with T cells and inflammatory myeloid DCs. *PLoS One*. 2012;7(2):e30308. doi:10.1371/journal.pone.0030308

57. Lowes MA, Chamian F, Abello MV, et al. Increase in TNF-alpha and inducible nitric oxide synthase-expressing dendritic cells in psoriasis and reduction with efalizumab (anti-CD11a). *Proc Natl Acad Sci USA*. 2005;102(52):19057–19062. doi:10.1073/pnas.0509736102

58. Frampton JE, Plosker GL. Efalizumab: a review of its use in the management of chronic moderate-to-severe plaque psoriasis. *Am J Clin Dermatol*. 2009;10(1):51–72. doi:10.2165/0128071-200910010-00009

59. Hyun YM, Choe YH, Park SA, Kim M. LFA-1 (CD11a/CD18) and Mac-1 (CD11b/CD18) distinctly regulate neutrophil extravasation through hotspots I and II. *Exp mol Med*. 2019;51(4):1–13. doi:10.1038/s12276-019-0227-1

60. Kamata M, Tada Y. Crosstalk: keratinocytes and immune cells in psoriasis. *Front Immunol*. 2023;14:1286344. doi:10.3389/fimmu.2023.1286344

61. Krapp C, Hotter D, Gawanbacht A, et al. Guanylate binding protein (GBP) 5 is an interferon-inducible inhibitor of HIV-1 infectivity. *Cell Host & Microbe*. 2016;19(4):504–514. *Cell Host Microbe*. doi:10.1016/j.chom.2016.02.019

62. Shenoy AR, Wellington DA, Kumar P, et al. GBP5 promotes NLRP3 inflammasome assembly and immunity in mammals. *Science*. 2012;336 (6080):481–485. doi:10.1126/science.1217141

63. Jia Y, Zhang L, Liu Z, et al. Targeting macrophage TFEB-14-3-3 epsilon interface by naringenin inhibits abdominal aortic aneurysm. *Cell Discov*. 2022;8(1):21. doi:10.1038/s41421-021-00363-1